




# Packaged whispering gallery resonator device based on an optical nanoantenna coupler

ANGZHEN LI,<sup>1,2</sup> KE TIAN,<sup>2</sup> JIBO YU,<sup>1,2</sup> RASHMI A. MINZ,<sup>3</sup>  
JONATHAN M. WARD,<sup>4</sup> SAMIR MONDAL,<sup>3</sup>  PENGFEI WANG,<sup>1,5,6</sup>   
AND SÍLE NIC CHORMAIC<sup>2,7</sup> 

<sup>1</sup>Key Laboratory of In-Fiber Integrated Optics of Ministry of Education, College of Science, Harbin Engineering University, Harbin 150001, China

<sup>2</sup>Light-Matter Interactions for Quantum Technologies Unit, Okinawa Institute of Science and Technology Graduate University, Onna, Okinawa 904-0495, Japan

<sup>3</sup>Central Scientific Instruments Organisation (Council of Scientific and Industrial Research, India), Chandigarh 160030, India

<sup>4</sup>Physics Department, University College Cork, Cork, Ireland

<sup>5</sup>Key Laboratory of Optoelectronic Devices and Systems of Ministry of Education and Guangdong Province College of Optoelectronic Engineering, Shenzhen University, Shenzhen 518060, China

<sup>6</sup>pengfei.wang@tudublin.ie

<sup>7</sup>sile.nicchormaic@oist.jp

**Abstract:** In this work, we present a packaged whispering gallery mode (WGM) device based on an optical nanoantenna as the coupler and a glass microsphere as the resonator. The microspheres were fabricated from either SiO<sub>2</sub> fiber or Er<sup>3+</sup>-doped fiber, the latter creating a WGM laser with a threshold of 93 μW at 1531 nm. The coupler-resonator WGM device was packaged in a glass capillary. The performance of the packaged microlaser was characterized, with lasing emission both excited in and collected from the WGM cavity via the nanoantenna. The packaged system provides isolation from environmental contamination, a small size, and unidirectional coupling while maintaining a high quality (Q-) factor (~10<sup>8</sup>).

© 2021 Optical Society of America under the terms of the [OSA Open Access Publishing Agreement](#)

## 1. Introduction

Whispering gallery mode (WGM) devices have shown great potential in many fields [1–8] and the optical coupler, a tool for transferring light in and out of the resonators [9–11], is a very important part of the WGM system. Among the various coupling schemes demonstrated, tapered fibers [11] are near ideal in terms of coupling efficiency because of their ability to achieve critical coupling [12] and the fact that they can be used to tailor the cavity input-output relations in the WGM resonator-waveguide system [13]. However, there are still issues with the tapered fiber coupling scheme, especially in terms of practical applications. First, tapered fibers are typically less than a few μm in diameter, making them extremely fragile. Second, the resonator-coupler system can be affected by environmental factors, which continuously and randomly change the coupling. Dust in the environment can also significantly reduce the quality (Q)-factors and efficiency of the coupling. These limitations can hinder practical applications of WGM resonators.

In the laboratory, the WGM system is usually placed in a closed chamber or in a clean room to isolate it from the environment. Several research works have focused on packaging the WGM system in a small enclosed space to shield it from air currents and pollution. For example, a packaging scheme consisting of two glass plates and a tube to fix the microsphere and tapered fiber relative to each other ensured that the cavity-fiber system moved as a whole while maintaining the Q-factor ( $1.08 \times 10^8$  at 1550 nm) [14]; however, it did not solve the problems of fiber fragility and environmental contamination. The scheme still relied on a suspended, several-centimeter-long

tapered fiber with a waist diameter of only  $2.5\ \mu\text{m}$  as the coupler. Moreover, the packaged device still had to be placed in a closed protective chamber [14].

Packaging resonator-tapered fiber systems with a low refractive index optical glue showed some promise toward solving the problem of fiber damage and contamination [15]. A low-index polymer packaged microtoroid-tapered fiber device with a Q-factor up to  $2 \times 10^7$  at 780 nm has been demonstrated [16]. However, this method degraded the Q-factors of the system [15–18]. Also, limited by the length of the tapered fiber, the size of such packaged devices is often on the centimeter scale [14,16,18]. Further downsizing of resonator-tapered fiber packaged devices is challenging.

In recent years, some embedded devices which do not use tapered fibers as couplers have been developed with the aim of overcoming the aforementioned challenges. For example, excitation and collection of the whispering gallery modes can be achieved using an etched thin-walled capillary [19], a tapered hollow annular core fiber [20], an embedded dual core hollow fiber [21] or a femtosecond laser-engraved waveguide [22] as a coupler. These embedded packaging solutions offer advantages in terms of system stability, smaller size, and immunity to environmental interference, but the Q-factors can be seriously affected. In contrast, our previous work [23] demonstrated coupling to WGM resonators using a nanoantenna based on Rayleigh scattering [24], while maintaining high Q-factors. Good coupling efficiency compared with other methods based on Rayleigh scattering was achieved.

Here, we propose and demonstrate a packaged WGM resonator using a fiber-based nanoantenna, similar to that presented in [23]. This small footprint, packaged device addresses environmental contamination while maintaining very high Q-factors of the order of  $10^8$  at 1531 nm pump. In addition, the nanoantenna structure allows for excitation and collection of signals using a single fiber probe, showing considerable promise in terms of practicality. Based on this scheme, we have also fabricated and packaged an  $\text{Er}^{3+}$ -doped WGM laser and its performance is studied and discussed. The demonstration of lasing in a packaged WGM device fabricated directly from Er-doped fiber is significant as it avoids the necessity of coating the resonator via solgel [25,26] or using other methods [27–29], thereby increasing the functionality of the device by reducing its complexity.

## 2. Device fabrication

There are several techniques used to make spherical WGM resonators [12,28,30–32]. One of the more common methods involves melting the end of a piece of optical fiber, using, for example, a  $\text{CO}_2$  laser [12] and we used this technique for the initial microsphere fabrication. Such microspheres have a fiber rod at the pole perpendicular to the equatorial plane where the resonance is formed. Although this rod does not affect the formation of the resonance at the equator, it poses difficulties for packaging and miniaturization of the device. To overcome this, here, we instigated an additional fabrication step in order to have a half-tapered fiber as a manipulation rod parallel to the resonance-forming surface. Figure 1 illustrates the process. The half-tapered fiber, with a small amount of UV curing glue on its tip, and a microsphere were fixed on two 3D stages. Under a microscope, the two 3D stages were adjusted to bring the tip of the half-tapered fiber into contact with the connecting point of the microsphere and its thin fiber rod (Fig. 1(a)). Next, the contact area was irradiated with UV light for a few seconds to cure the UV glue (Fig. 1(b)). After curing, the microsphere was torn from its original rod by moving the 3D stage. For this to work, the half-tapered fiber must be thicker than the microsphere's intrinsic fiber rod to facilitate breakage when moving the stage. Now the microsphere has a supporting rod parallel to the resonance plane (Fig. 1(c)). In this experiment, the fiber used to prepare both the microsphere and the half-tapered fiber was a commercial silica fiber (1060XP, Thorlabs).

To fabricate the nanoantenna for optical coupling to the microsphere, we chemically etched photosensitive optical fiber (GF3, Nufern), using a technique developed by Mondal *et al.*, as

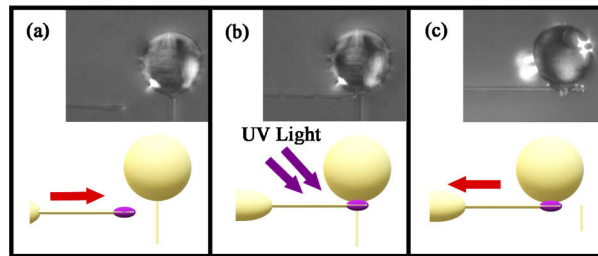


**Fig. 1.** Mounting a microsphere to a connecting rod. (a) Approach a half-tapered optical fiber coated with UV glue to the connection point between the microsphere and the connecting rod. (b) Fix the half-taper at the connection point under UV light. (c) Tear the microsphere free from the original fiber rod by adjusting the position of the 3D stage.

reported in [33,34]. For this particular fiber, the fiber core etches quicker than the cladding under the same hydrofluoric (HF) acid etching conditions. The first step in the preparation process was to remove the coating from one end of the fiber and cut the end face flat. It was then secured in a vertical position with a micrometer-adjustable fiber optic holder. A small plastic vial containing 48% HF acid solution was fixed directly below the optical fiber. An oil film on the surface of the acid solution prevented evaporation. The etching process was divided into two steps. First, the position of the fiber holder was adjusted so that the end face of the fiber just touched the surface of the acid. Under the action of liquid surface tension, the acid rose up along the outer wall of the fiber and etched the cladding and core simultaneously (Fig. 2(a)). After 30 minutes, the core inside the fiber formed a tiny tip (Fig. 2(b)). The second step involved adjusting the holder to move the fiber down into the acid by about  $20\ \mu\text{m}$  (Fig. 2(c)). The elevated height of the acid level and the difference between the etching rates of the cladding and core materials created a capillary ring at the core-cladding boundary.

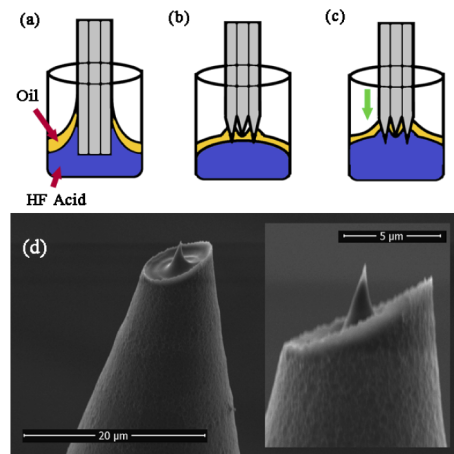


**Fig. 2.** Fabrication of a nanoantenna. (a) The end face of the fiber is brought into contact with the HF acid surface. Under the action of liquid surface tension, HF acid rises up along the outer wall of the fiber and etches the cladding and core. (b) After 30 minutes, the core inside the fiber forms a tiny tip. Because the core is etched faster than the cladding, the sample has a ring tube formed by cladding that is longer than the tip. (c) Moving the sample down  $20\ \mu\text{m}$  and continue etching for 10 minutes. (d) A scanning electron microscope (SEM) image of a fabricated nanoantenna.

After about 10 minutes of etching, an antenna with a protruding nanoprobe was obtained. The etched sample was cleaned with acetone to remove the oil layer on the surface of the nanoantenna. A scanning electron microscope (SEM) image of a fabricated nanoantenna is shown in Fig. 2(d). Finally, the nanoantenna and the microsphere were inserted into a capillary using 3D stages (Fig. 3(a)). After adjusting their relative positions under a microscope, while monitoring the WGM spectrum, the two sides of the capillary were sealed with UV glue and irradiated by UV light (Fig. 3(b)). This ensured that the whole WGM system was contained within a small enclosed space and that the coupling gap did not change after the packaging process (Fig. 3(b)). The coupling and mode shape could still be adjusted by changing the polarization [23]. Figure 3(c) shows a prepared sample with a microsphere diameter of  $160\ \mu\text{m}$  packaged in a capillary with  $350\ \mu\text{m}$  outer diameter and  $250\ \mu\text{m}$  inner diameter. The fiber on one side of the nanoantenna acts as a waveguide for the output and input optical signals, while the pigtail fiber on the other side, which is connected to the microsphere, can be cut off if desired.

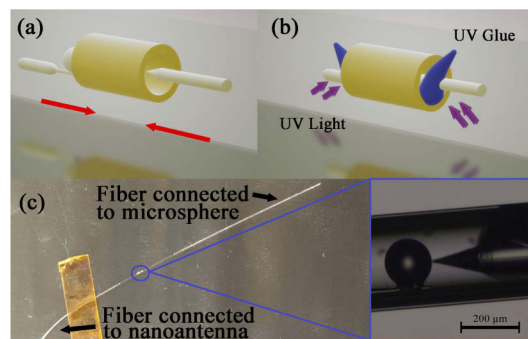


**Fig. 3.** Packaging process. (a) The microsphere and nanoantenna are inserted into a short capillary tube and adjusted in position. (b) The two sides of the capillary are sealed with UV glue and irradiated by UV light (c) A packaged device. The zoomed-in image shows a packaged structure in detail.

### 3. Results and discussion

A schematic of the experimental setup to test the performance of the packaged devices is shown in Fig. 4. Pump light at  $1531\ \text{nm}$  was coupled to the microsphere via the nanoantenna. A 3-port circulator was used to separate the input and collected signals. A half-wave plate on the input beam was used for polarization adjustment. The signal was transmitted from the output of the circulator and observed on an oscilloscope (WaveSurfer 10, Teledyne LeCroy) and an optical spectrum analyzer (MS9740B, Anritsu).

The pump source was a tunable laser (TLB 6700, Newport) operating near  $1531\ \text{nm}$ . Through excitation via the nanoantenna, we observed a WGM spectrum containing multiple resonances (Fig. 5(a)). Four typical resonances are labeled in the spectrum as A, B, C, and D, and their details are shown in Fig. 5(b)-(e), respectively. We see that A is a typical Fano resonance ( $Q_A = 1.1 \times 10^8$ ) formed by a continuous spectrum corresponding to the field reflected from the surface of the sphere and a discrete spectrum corresponding to the scattering cavity field [35]. The modes B, C, and D correspond to three typical Lorentz peaks or dips and their Q-factors are  $Q_B = 1.0 \times 10^8$ ,  $Q_C = 1.7 \times 10^8$  and  $Q_D = 0.6 \times 10^8$ , respectively. Compared with our previous work [23], we observed that the resonator maintained high a Q-factor after packaging. The optical coupling was also not affected by the packaging method since the UV glue was far removed from the coupling region. We conclude that the packaging technique did not degrade the performance of the system in contrast to other WGM packaging methods [15–22].

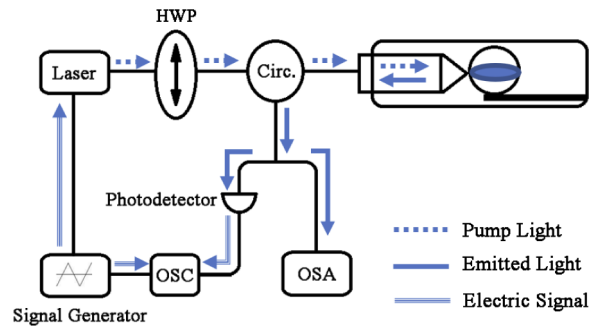


**Fig. 4.** Schematic of the test system. OSC: Oscilloscope; OSA: Optical spectrum analyzer; HWP: Halfwave plate; Circ.: Circulator.

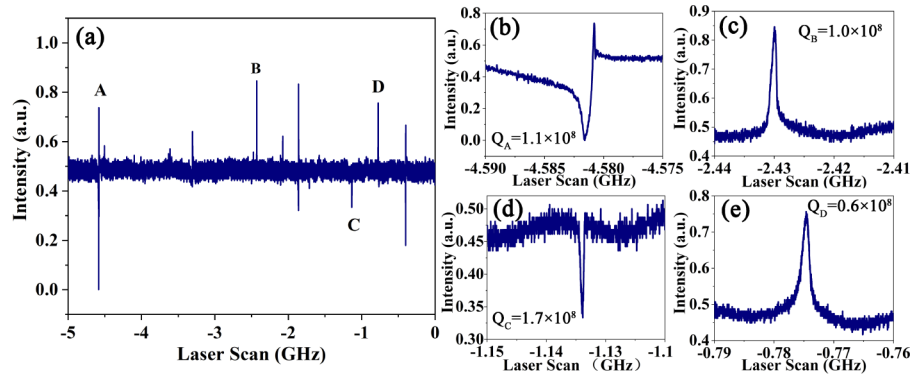


**Fig. 5.** WGM spectra for the packaged device. (a) Reflection spectrum using a 1531 nm tunable laser. (b)-(e) Details of the four labeled resonances in the reflection spectrum.

We also prepared an active packaged device following the same method as described for the passive device but using  $\text{Er}^{3+}$ -doped fiber (M12-980-125, Thorlabs) to make the microspheres. When 1531 nm pump light was coupled into the resonator via the nanoantenna, lasing behavior was observed at 1558 nm. The pump laser was kept at a fixed frequency during this experiment; in other words, the pump/cavity resonance overlap was coincidental. Rotating the polarization could improve or degrade the coupling depending on the initial conditions, such as detuning and degree of polarization. Pumping the WGM cavity in this way illustrated that we could achieve relatively low-threshold lasing even without controlling the aforementioned parameters.

Figure 6(a) shows the output laser spectrum for different pump powers ranging from 0.85 mW to 5.63 mW. Note that the pump power is measured at the input end of the nanoantenna fiber. The relationship between the pump power and the lasing output power is shown in Fig. 6(b). The launched pump power at lasing threshold is less than 0.85 mW and the laser power shows a linear relationship with the pump power above threshold. The launched pump power is of the same order as that recorded (0.485 mW) for lasing in a WGM resonator by pumping via a Rayleigh scatter [36]. In our experiment, the laser displayed single-mode behavior without any sign of saturation when the pump power was increased to 5.63 mW. At this input power, the back-reflected pump power measured at the input to the OSA was  $7.7 \mu\text{W}$ . Assuming the input and output coupling strengths are equal, this equates to a coupling efficiency of 11.4%, similar to the unpackaged system we reported on previously [23]. At threshold, we would expect the input power to be  $93 \mu\text{W}$ . Threshold could be lowered by locking the pump laser to a WGM or optimizing the pump polarization and nanoantenna position.



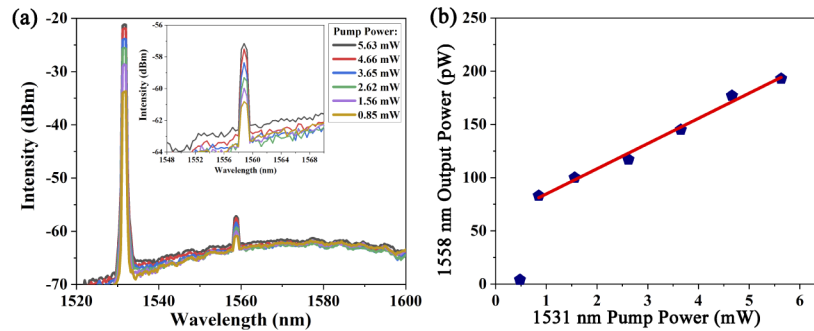


**Fig. 6.** Laser performance of an  $\text{Er}^{3+}$ -doped packaged microsphere device. (a) The laser spectrum at different 1531 nm pump powers. The lasing emission is centered on 1558 nm. (b) Output laser power at 1558 nm as a function of 1531 nm pump power light. Blue dots: experimental data; Red line: linear fit. The lasing threshold is at around 0.85 mW.

#### 4. Conclusion

In conclusion, we have designed and fabricated a packaged WGM device based on a fiber nanoantenna as a coupler for both a passive and an active microsphere resonator. The device has the advantages of having a small footprint and good resistance to environmental interference and pollution whilst maintaining high Q-factors of the order of  $10^8$  for the passive devices. Since the Rayleigh scattering coupling mechanism does not rely on phase matching [37] this scheme could, in principle, be used to fabricate packaged WGM devices from a range of different materials, such as multicomponent glasses, crystals, etc. Another important point is that the nanoantenna can achieve Rayleigh-induced coupling without depositing a scatterer onto the surface of the WGM resonator — a non-trivial task if one wishes to do so in a deterministic manner. The point-and-play feature of the nanoantenna simplifies the coupling method significantly. In summary, this work offers a reliable way to provide environmental isolation, increased robustness, and portability to WGM resonators. This should pave the way to move WGM resonators from the laboratory to the field for a variety of applications such as low threshold lasers, filters, and sensors.

**Funding.** National Key Program of the National Natural Science Foundation of China (61935006, 62090062); China Scholarship Council (201906680065); 111 Project to the Harbin Engineering University (B13015); Okinawa Institute of Science and Technology Graduate University; Science and Engineering Research Board (CRG/2019/001215); Indian Council of Medical Research (5/3/8/12/ITR-F/2020-ITR).

**Acknowledgments.** The authors acknowledge the Engineering Support Section of OIST Graduate University.

**Disclosures.** The authors declare no conflicts of interest.

#### References

1. A. A. Savchenkov, A. B. Matsko, V. S. Ilchenko, I. Solomatine, D. Seidel, and L. Maleki, "Tunable optical frequency comb with a crystalline whispering gallery mode resonator," *Phys. Rev. Lett.* **101**(9), 093902 (2008).
2. J. Zhu, S. K. Özdemir, Y. F. Xiao, L. Li, L. He, D. R. Chen, and L. Yang, "On-chip single nanoparticle detection and sizing by mode splitting in an ultrahigh-Q microresonator," *Nat. Photonics* **4**(2), 122 (2010).
3. J. U. Füst, D. V. Strekalov, D. Elser, A. Aiello, U. L. Andersen, C. Marquardt, and G. Leuchs, "Quantum light from a whispering-gallery-mode disk resonator," *Phys. Rev. Lett.* **106**(11), 113901 (2011).
4. F. Monifi, S. Kaya Özdemir, and L. Yang, "Tunable add-drop filter using an active whispering gallery mode microcavity," *Appl. Phys. Lett.* **103**(18), 181103 (2013).
5. Y. Yang, Y. Ooka, R. M. Thompson, J. M. Ward, and S. Nic Chormaic, "Degenerate four-wave mixing in a silica hollow bottle-like microresonator," *Opt. Lett.* **41**(3), 575–578 (2016).
6. Z. Fang, S. Nic Chormaic, S. Wang, X. Wang, J. Yu, Y. Jiang, J. Qiu, and P. Wang, "Bismuth-doped glass microsphere lasers," *Photonics Res.* **5**(6), 740–744 (2017).
7. J. M. Ward, Y. Yang, F. Lei, X.-C. Yu, Y.-F. Xiao, and S. Nic Chormaic, "Nanoparticle sensing beyond evanescent field interaction with a quasi-droplet microcavity," *Optica* **5**(6), 674–677 (2018).

8. L. T. Hogan, E. H. Horak, J. M. Ward, K. A. Knapper, S. Nic Chormaic, and R. H. Goldsmith, "Toward real-time monitoring and control of single nanoparticle properties with a microbubble resonator spectrometer," *ACS Nano* **13**(11), 12743–12757 (2019).
9. Y.-L. Pan and R. K. Chang, "Highly efficient prism coupling to whispering gallery modes of a square  $\mu$  cavity," *Appl. Phys. Lett.* **82**(4), 487–489 (2003).
10. R. Dong, A. J. Qavi, J. Liao, and L. Yang, "Angle-polished fibers as a robust coupling tool for photonics," in *Chemical, Biological, Radiological, Nuclear, and Explosives (CBRNE) Sensing XX*, vol. 11010 J. A. Guicheteau and C. R. Howle, eds., International Society for Optics and Photonics (SPIE, 2019), pp. 290–296.
11. J. C. Knight, G. Cheung, F. Jacques, and T. A. Birks, "Phase-matched excitation of whispering-gallery-mode resonances by a fiber taper," *Opt. Lett.* **22**(15), 1129–1131 (1997).
12. M. Cai, O. Painter, and K. J. Vahala, "Observation of critical coupling in a fiber taper to a silica-microsphere whispering-gallery mode system," *Phys. Rev. Lett.* **85**(1), 74–77 (2000).
13. F. Lei, J. M. Ward, P. Romagnoli, and S. Nic Chormaic, "Polarization-controlled cavity input-output relations," *Phys. Rev. Lett.* **124**(10), 103902 (2020).
14. Y. Dong, K. Wang, and X. Jin, "Packaged microsphere-taper coupling system with a high Q factor," *Appl. Opt.* **54**(2), 277–284 (2015).
15. Y.-Z. Yan, C.-L. Zou, S.-B. Yan, F.-W. Sun, Z. Ji, J. Liu, Y.-G. Zhang, L. Wang, C.-Y. Xue, W.-D. Zhang, Z.-F. Han, and J.-J. Xiong, "Packaged silica microsphere-taper coupling system for robust thermal sensing application," *Opt. Express* **19**(7), 5753–5759 (2011).
16. V. Kavungal, G. Farrell, Q. Wu, A. K. Mallik, and Y. Semenova, "A packaged whispering gallery mode strain sensor based on a polymer-wire cylindrical micro resonator," *J. Lightwave Technol.* **36**(9), 1757–1765 (2018).
17. P. Wang, R. Madugani, H. Zhao, W. Yang, J. M. Ward, Y. Yang, G. Farrell, G. Brambilla, and S. Nic Chormaic, "Packaged optical add-drop filter based on an optical microfiber coupler and a microsphere," *IEEE Photonics Technol. Lett.* **28**(20), 2277–2280 (2016).
18. G. Zhao, T. Wang, L. Xu, E. King, G.-L. Long, and L. Yang, "Raman lasing and Fano lineshapes in a packaged fiber-coupled whispering-gallery-mode microresonator," *Sci. Bull.* **62**(12), 875–878 (2017).
19. X. Q. Bai and D. N. Wang, "Whispering-gallery-mode excitation in a microsphere by use of an etched cavity on a multimode fiber end," *Opt. Lett.* **43**(22), 5512–5515 (2018).
20. J. Wang, X. Zhang, M. Yan, L. Yang, F. Hou, W. Sun, X. Zhang, L. Yuan, H. Xiao, and T. Wang, "Embedded whispering-gallery mode microsphere resonator in a tapered hollow annular core fiber," *Photonics Res.* **6**(12), 1124–1129 (2018).
21. M. Zhang, W. Yang, K. Tian, J. Yu, A. Li, S. Wang, E. Lewis, G. Farrell, L. Yuan, and P. Wang, "In-fiber whispering-gallery mode microsphere resonator-based integrated device," *Opt. Lett.* **43**(16), 3961–3964 (2018).
22. X. Liu, X. L. Cui, and D. N. Wang, "Integrated in-fiber coupler for a whispering-gallery mode microsphere resonator," *Opt. Lett.* **45**(6), 1467–1470 (2020).
23. J. M. Ward, F. Lei, S. Vincent, P. Gupta, S. K. Mondal, J. Fick, and S. Nic Chormaic, "Excitation of whispering gallery modes with a "point-and-play," fiber-based, optical nano-antenna," *Opt. Lett.* **44**(13), 3386–3389 (2019).
24. F. Shu, X. Jiang, G. Zhao, and L. Yang, "A scatterer-assisted whispering-gallery-mode microprobe," *Nanophotonics* **7**(8), 1455–1460 (2018).
25. L. Yang and K. J. Vahala, "Gain functionalization of silica microresonators," *Opt. Lett.* **28**(8), 592–594 (2003).
26. Y. Yang, F. Lei, S. Kasumie, L. Xu, J. M. Ward, L. Yang, and S. Nic Chormaic, "Tunable erbium-doped microbubble laser fabricated by sol-gel coating," *Opt. Express* **25**(2), 1308–1313 (2017).
27. C. Dong, Y. Xiao, Z. Han, G. Guo, X. Jiang, L. Tong, C. Gu, and H. Ming, "Low-threshold microlaser in Er:Yb phosphate glass coated microsphere," *IEEE Photonics Technol. Lett.* **20**(5), 342–344 (2008).
28. S. Chen, T. Sun, K. Grattan, K. Annapurna, and R. Sen, "Characteristics of Er and Er-Yb-Cr doped phosphate microsphere fibre lasers," *Opt. Commun.* **282**(18), 3765–3769 (2009).
29. J. Ward, Y. Yang, and S. Nic Chormaic, "Glass-on-glass fabrication of bottle-shaped tunable microlasers and their applications," *Sci. Rep.* **6**(1), 25252 (2016).
30. F. Lissillour, K. A. Ameer, N. Dubreuil, G. M. Stephan, and M. Poulain, "Whispering-gallery-mode Nd:ZBLAN microlasers at 1.05  $\mu\text{m}$ ," in *Infrared Glass Optical Fibers and Their Applications*, vol. 3416 M. Saad, ed., International Society for Optics and Photonics (SPIE, 1998), pp. 150–156.
31. J. M. Ward, Y. Wu, K. Khalfi, and S. Nic Chormaic, "Short vertical tube furnace for the fabrication of doped glass microsphere lasers," *Rev. Sci. Instrum.* **81**(7), 073106 (2010).
32. R. Madugani, Y. Yang, J. M. Ward, J. D. Riordan, S. Coppola, V. Vespini, S. Grilli, A. Finizio, P. Ferraro, and S. Nic Chormaic, "Terahertz tuning of whispering gallery modes in a PDMS stand-alone, stretchable microsphere," *Opt. Lett.* **37**(22), 4762–4764 (2012).
33. S. K. Mondal, A. Mitra, N. Singh, S. N. Sarkar, and P. Kapur, "Optical fiber nanoprobe preparation for near-field optical microscopy by chemical etching under surface tension and capillary action," *Opt. Express* **17**(22), 19470–19475 (2009).
34. S. K. Mondal, A. Mitra, N. Singh, F. Shi, and P. Kapur, "Ultrafine fiber tip etched in hydrophobic polymer coated tube for near-field scanning plasmonic probe," *IEEE Photonics Technol. Lett.* **23**(19), 1382–1384 (2011).
35. F.-J. Shu, C.-L. Zou, and F.-W. Sun, "Perpendicular coupler for whispering-gallery resonators," *Opt. Lett.* **37**(15), 3123–3125 (2012).

36. J. Zhu, S. K. Özdemir, H. Yilmaz, B. Peng, M. Dong, M. Tames, T. Carmon, and L. Yang, "Interfacing whispering-gallery microresonators and free space light with cavity enhanced rayleigh scattering," *Sci. Rep.* **4**(1), 6396 (2015).
37. A. B. Matsko and V. S. Ilchenko, "Optical resonators with whispering-gallery modes-part I: basics," *IEEE J. Sel. Top. Quantum Electron.* **12**(1), 3–14 (2006).